Supplemental Data

Supplemental Figure 1.

(A, B) In WT, LOV-1::GFP is found in cell bodies of CEM and RnB neurons and cilia of CEM neurons. Only one CEM cilium is brightly labeled with LOV-1::GFP, probably due to low LOV-1::GFP expression levels or mosaicism. (C) In *cil-1(my15)* CEMs, LOV-1::GFP is visible in dendrites and axons as well as cell bodies. (D) In *cil-1(my15)* RnBs, LOV-1::GFP is found in dendrites and cell bodies. (E, F) P*pkd-2*::SNB-1(Synaptobrevin)::GFP in CEM neurons of both WT and *cil-1(my15)* animals localizes to the axonal processes. (G) Mating behavioral efficiency of WT (*him-5(e1490)*), *pkd-2(sy606); him-5(e1490)*, and *cil-1(my15); him-5(e1490)*. *cil-1; him-5* males exhibit WT behaviors in three steps during mating behaviors (response, vulva location, and spicule insertion/initiation of sperm transfer). Response and vulva location steps require *pkd-2* and *lov-1*.

Supplemental Figure 2. Phylogenetic analysis on 5-phosphatases

(A) Phylogenetic analysis of 5-phosphatase family. The NJ tree based on the analysis of the catalytic domain of inositol 5-phosphatase protein sequences encoded in the genomes of five animals and three related unicellular eukaryotes. Type I sequences were excluded in the analysis due to their low sequence similarity to the sequences of interest. Although the catalytic domain sequences of the RhoGAP domain-containing inositol 5-phosphatases of *C. elegans* and *D. melanogaster* did not form a clade with the other Type II/OCRL sequences, they nevertheless share several amino acids within a hypervariable region, suggesting they are derived from a common ancestor. Catalytic domains are highly homologous between CIL-1 and T25B9.10, but the latter lacks the SKICH-like domain. The tree is arbitrarily rooted. Bootstrap support values

(NJ/MP) over 50% are shown at the corresponding nodes. Note that the presence of characteristic domains is indicated with symbols as designated in rectangular boxes. (B) Two conserved sequence motifs of 5-phosphatases. Representative members of each subfamily and SKICH-like member are aligned. Pink vertical boxes indicate residues with absolute conservation including CIL-1. Four residues with arrows are essential residues for 5-phosphatase catalytic activity. The residue in red (N) was substituted to A to create the phosphatase-DEAD CIL-1 construct. (C) Predicted phylogenetic relationships among eight organisms included in the study [1, 2]. Note that relationships among nematodes (e.g., *C. elegans*), arthropods (e.g., *D. melanogaster*), and deuterostomes (e.g., vertebrates) remain controversial (dotted line) [3, 4]. (D) SKICH-like domain alignment. Pink vertical boxes indicate identified residues in mammalian PIPP and SKIP [5] and gray boxes include residues with reported similarities between mammalian members. Open boxes indicate additional homologous sequences. The CIL-1 SKICH-like domain is slightly divergent.

Supplemental Figure 3. *cil-1* expression and localization

(A-C) The GFP expression driven by a 2.2kb *bath-42* promoter (P*bath-42*(2.2kb)::GFP) is broad in both hermaphrodites and males. In adult hermaphrodite head (A), adult male head (B), and tail (C), the 2.2kb *bath-42* promoter is expressed in the pharynx (ph), intestine (in), and unidentified neurons (n). (D-E) P*pkd-2*::CIL-1::tdTomato in male head (D) and tail (E). The tdtomato labels cilia (arrowheads), dendrites (den), axon, and small spots in cell bodies (arrows). (F) Intestinal expression of CIL-1 labels reticular structure in the cytoplasm (arrows). Scale bar, 10um.

Supplemental Figure 4. PI and early endosomal markers in male specific sensory neurons. Arrows indicate the location of cell bodies. (A-B) P*pkd-2*::AKT(PH)::GFP as a PI(3,4,5)P3/PI(3,4)P3 marker male tail. (A) PI(3,4,5)P3/PI(3,4)P3 in WT male tail neurons is primarily visible on cell surface. (B) In *cil-1(my15)*, PI(3,4,5)P3/PI(3,4)P3 is similarly distributed along the plasma membrane in male tail neurons. (C-D) P*pkd-2*::PLCδ(PH)::GFP labels PI(4,5)P2 in male tail neurons. In both WT (C) and *my15* (D) neurons, PI(4,5)P2 is evenly distributed in the cell surface. (E-F) P*pkd-2*::FYVEx2::GFP as a PI(3)P marker. (E) In WT, PI(3)P is bright in the nuclei (arrows, big spots) and small compartments supposedly early endosomes, but rarely visible in dendritic processes or cilia. (F) In *my15*, PI(3)P is similarly bright in the nuclei (arrows), but distinctly labels distal dendrites and cilia (arrowheads). (G-H) P*pkd-2*::mRFP::RAB-5 labels early endosomes (arrows, small spots) and smoothly along the dendrites (den) both in WT (G) and *my15* (H) male tail neurons. (J-I) Similarly, P*pkd-2*::STAM-1::mRFP is visible in early endosomes (arrows) and dendrites (den) in WT (J) and *my15* (I) background.

Supplemental Figure 5. *cil-1(my15)* mutants are semi sterile due to sperm defects (A) Semi-sterility in *cil-1(my15); him-5(e1490).* *my15* hermaphrodites have a reduced brood size at 20 degree compared to WT. (B) *my15* hermaphroditic sterility can be rescued by mating with WT males. (C) *my15* males exhibit a low Mating Efficiency (% of cross progeny over total progeny), measuring males' ability to sire cross progeny. When mated with *my15* males, the number of total progeny is not suppressed, indicating that sperm from *my15* males do not compete with endogenous hermaphrodite-derived sperm. (D-E) DAPI stained adult hermaphrodites. (D) In a WT hermaphrodite, the gonad contains developing embryos

(arrowheads). Spt; location of the spermatheca. (E) *my15* hermaphrodites contain endomitotic oocytes (arrowheads) in the uterus, showing large DAPI positive spots. Progression of germline development appears normal both in *my15* hermaphrodites and male; however, the morphology of germline tube may be mildly affected, suggesting pleiotropic roles of *cil-1*. Panel D and E are images of young adult hermaphrodites under the same magnification. In E, however, the *my15* unfertilized oocytes are prominent (arrowheads) and the *my15* gonad appears slightly narrower than WT, possibly due to massive unfertilized oocyte accumulation or unknown *cil-1* function in maintaining healthy gonad architecture. We would like to clarify that progression of spermatogenesis and oogenesis are unaffected in *my15* mutants. Scale bar, 50 um. (F-G) Nomarski (differential interference contrast (DIC)) images of WT and *my15* hermaphrodite uterus. Spermatheca (not shown) to the left, vulva to the right as indicated. (F) The WT hermaphrodite uterus contains a zygote, 2-cell and 4-cell embryo, which are encapsulated with eggshell (arrowheads). (G) In the *my15* hermaphrodite uterus, endomitotic cells are identified by large nuclei (arrowheads), lack of eggshell, and irregular shapes. Scale bar, 10 um.

Supplemental Movie 1. PKD-2::GFP motility in dendrites of a WT CEM neuron. PKD-2::GFP particles move bidirectionally along the WT dendrite. Anterior (towards cilia) on left. Speed x6.

Supplemental Movie 2. PKD-2::GFP motility in a *cil-1(my15)* CEM dendrite. Motile PKD-2::GFP particles are visible along *my15* dendrite with increased PKD-2::GFP (Cil phenotype). Speed x6.

Supplemental Movie 3. Chemically activated WT sperm crawl on a glass slide after 9 minutes into activation. Speed 10x, elapsed time is indicated in seconds.

Supplemental Movie 4. Chemically activated *cil-1(my15)* sperm display diminished motility. The movie starts at 9 minutes after monensin application. Speed 10x, elapsed time is indicated in seconds.

EXPERIMENTAL PROCEDURES

C. elegans strains and genetics

Nematodes were raised under standard conditions [6]. "WT (wild type)" or "WT control" refers to *him-5(e1490)V* for high incidence of males [7]. Transgenic animals were generated by germline injections [8]. The recessive mutation *my15* was isolated in a genetic screen [9]. *cil-1(my15)* was outcrossed six times. For deficiency tests, MT3022 (*nDf20/sma-2(e502*) *unc-32(e189)*III) heat-shock induced males were crossed with *unc-32 my15* III*; pkd-2(sy606) myIs1* [PKD-2::GFP; Pcoelomocyte::GFP] IV*; him-5(e1490)* V [10]. Non-Unc F1 males (*unc-32 my15/nDf20* III*; pkd-2/+ myIs1/+* IV*; him-5/+* V were scored for PKD-2::GFP localization. Non-Unc F1 hermaphrodites were examined for self-fertility. For SNP mapping, *dpy-17 my15 unc-32* III; *pkd-2 myIs1* IV*; him-5* V (Unc Dpy) hermaphrodites were crossed with males from CB4856 Hawaiian strain. In F2s, either NonUnc Dpy or Unc NonDpy recombinant hermaphrodites were singled out to score Cil (in F3 males) and Spe (F2 semi-sterility) phenotypes.

A combination of three point and single nucleotide polymorphism (SNP) mapping placed the *cil-1* locus between snp_C14B9[1] and snp_C02F5 on the linkage group III. *my15/my15* and *my15*/*nDf20* are phenotypically indistinguishable in Cil and Spe phenotypes, indicating that *my15* is a null or reduction of function allele.

Molecular cloning

Restriction fragment and Gateway cloning (Invitrogen) methods were used to generate plasmids for fluorescent protein fused markers, which include GFP (green fluorescent protein), mRFP (monomeric) and tdtomato (tandem dimer tomato) (Clontech, [11]). For rescuing experiments, a series of PCR amplified genomic fragments along with the dominant *rol-6* marker [12] at 60ng/ul each were injected individually or in pools into WT animal and resulting transgenic lines were crossed into *my15* animals to score rescue of PKD-2::GFP mislocalization (Cil phenotype) and/or the spermatogenesis-defective (Spe phenotype) (Figure 3A). The genomic coordinates for fragments mentioned in Figure 2 are; 8150K: III: 8,146,448 to 8,155,624, 8160K: III: 8,154,210 to 8,164,811, 8160K-1: III: 8,158,952 to 8,164,811. To create PCR-SOEd products, the *bath-42* promoter was amplified by 5'ACTCACTGCTTTCAAGTTGCTGA3' and 5'*AGTCGATCGATGCCTCGA*TACCTCTGTTGATAAGTTGAGCGAG3'. The *cil-1* genomic region was amplified by 5' *TCGAGGCATCGATCGACT*ATAACAATGGATTGGAAAATAACAATATTC3' and 5'TGCAAGACTATTAGGGAGTG3'. The linker is italicized. The *my15* lesion was identified by sequencing using 5'AGGAGCCGTACTTACATGG3' (sense) and 5'AATTTGCCGCGTCGAGAC3' (antisense).

To determine *cil-1* expression pattern, a 2.2 or 1.5kb 5'UTR of *bath-42,* the gene upstream of *cil-1* in the operon, was used to drive GFP expression. P*bath-42*::GFP promoter fusions are broadly expressed in a highly mosaic manner including the intestine, pharynx, unidentified head and male tail neurons, body wall muscles, and hypodermis, but are not overlapping with *pkd-2* (Suppl. Figure 2A-C). Moreover, P*bath-42*::CIL-1::GFP expression does not rescue the *my15* Cil phenotype (data not shown), while a *cil-1(+)* genomic fragment

containing the C50G3.7 250 bp 5'UTR, genomic region, and 200bp 3'UTR partially rescues the *my15* Cil phenotype (Figure 3B). These data indicate that 5' UTR and 3'UTR of *cil-1*, and the 5'UTR of the operon coordinate *cil-1* expression.

Microscopy

Epifluorescence and Nomarski analyses were performed on a Zeiss Axioplan2 imaging system equipped with 10x, 63x (NA 1.4), 100x (NA 1.4) objectives and a Photometrics Cascade 512B CCD camera using Metamorph software. 3D deconvolution of Z-stacks of epifluorescent image were performed by AutoQuantX program (MediaCybernetics). Confocal images were collected using a 510 LSM META ZEISS. Optical sections were collected between 0.4-1.0 μm and projected as Z-series that were stored as TIFF files and manipulated using Adobe PhotoShop™. Worms were anesthetized with 1 mM levamisole, mounted on agar pads and maintained at room temperature. For time-lapse microscopy of sperm motility, Nomarski images were taken every 15 seconds for up to 15 minutes. Neuronal images shown in figures are projected epifluorescent Z-stacks after 3D deconvolution except for Figure 2C and 2G, which are projected Z-stacks of confocal sections. For electron microscopy, sperm were prepared essentially as described by [13], except that the samples were embedded in LX112 (Ladd Research Industries Inc., Burlington, VA).

Behavioral assays

Male behavioral assays (response and location of vulva efficiency) were performed as described [14, 15]. At least 20 males per genotype were scored per assay. Response efficiency reflects the percentage of the males that responded to the hermaphrodites within 4 minutes. Location of

vulva efficiency was calculated by successful vulva location divided by the total number of vulva encounters for each male. Spicule insertion efficiency was determined by the fraction of males that successfully insert the spicule during 15 minutes of observation with 3-day old *unc-31* hermaphrodites. Statistical analyses were performed by t-tests with two-tailed p-value. Mating efficiency was performed as described [16]. For sperm tracking assays, we isolated L4 males for 2 days and soaked in 1μg/ml MitoTracker Red CMXRos (Invitrogen) in M9 solution for 30 minutes (modified from [17]). After recovery on NGM plates, four males and three *unc-31* hermaphrodites are placed on each plate. For brood size, a single L4 hermaphrodite was isolated to a plate and kept at 20 degrees. The number of F1s was counted until the hermaphrodite stopped laying eggs. Dye filling, diacetyl olfaction, and osmotic avoidance assays were performed according to [16, 18].

Sperm isolation and activation

To isolate spermatids, virgin L4 males were isolated for 2-3 days in 20 degrees and cut with a 25g needle on a glass slide in Sperm Media (SM) pH 7.9 with 10mM Dextrose as described in [19, 20]. For in vitro activation, 20 ug/ml of Pronase or 100nM monensin (for in vitro sperm crawling experiments) was added to SM as described in [21]. For wortmannin treatment, a 100X wortmannin stock solution in DMSO was added to reach the final concentration of 100nM into SM.

Immunohistochemistry

For whole animal fixation, animals were washed free of bacteria in M9 and placed on poly-L-lysine coated slides in 2-3ul of PBS pH 7.4 containing 4% paraformaldehyde for 5 minutes at

room temperature [22]. A cover slip was put on the slide, it was placed onto a metal block cooled by dry ice for 20 minutes and then the coverslip was popped off with a razor blade. The slide was transferred to a containing -20^{o} methanol for 15 minutes, rehydrated in PBS and either antibody or DAPI staining was performed [22]. For isolated sperm immunochemistry, before and after adding in vitro activator, a 4X formaldehyde solution was added to a final concentration of 4%, followed by conventional immunohistochemistry methods.

Phylogenetic analysis of 5-phosphatases PI 5-phosphatase sequences obtained from GenBank or Wormbase included three vertebrates (*Homo sapiens*, *Mus musculus*, *Danio rerio*), two invertebrates (*Drosophila melanogaster*, *Caenorhabditis elegans*), and three unicellular eukaryotes (*Monosiga brevicollis*, *Saccharomyces cerevisiae*, *Dictyostelium discoideum*) (Suppl. Figure 1A) [2, 23]. 5-phosphatase catalytic domains were aligned using MacClade ver. 4.08 [24]. A total of 261 unambiguously aligned amino acid positions were included in the final alignment. Due to highly derived sequence nature, the Type I-like inositol 5-phosphatase sequences were excluded in phylogenetic analyses. Phylogenetic analysis was performed using PAUP* ver. 4.0 [25]. Neighbor joining and maximum parsimony trees were constructed and bootstrap values were obtained by 100 re-samplings.

References

1. Ruiz-Trillo, I., Roger, A.J., Burger, G., Gray, M.W., and Lang, B.F. (2008). A phylogenomic investigation into the origin of metazoa. Mol Biol Evol *25*, 664-672.
2. Baldauf, S.L., Roger, A.J., Wenk-Siefert, I., and Doolittle, W.F. (2000). A kingdom-level phylogeny of eukaryotes based on combined protein data. Science *290*, 972-977.
3. Rogozin, I.B., Wolf, Y.I., Carmel, L., and Koonin, E.V. (2007). Analysis of rare amino acid replacements supports the Coelomata clade. Mol Biol Evol *24*, 2594-2597.
4. Irimia, M., Maeso, I., Penny, D., Garcia-Fernandez, J., and Roy, S.W. (2007). Rare coding sequence changes are consistent with Ecdysozoa, not Coelomata. Mol Biol Evol *24*, 1604-1607.
5. Gurung, R., Tan, A., Ooms, L.M., McGrath, M.J., Huysmans, R.D., Munday, A.D., Prescott, M., Whisstock, J.C., and Mitchell, C.A. (2003). Identification of a novel domain in two mammalian inositol-polyphosphate 5-phosphatases that mediates membrane ruffle localization. The inositol 5-phosphatase skip localizes to the endoplasmic reticulum and translocates to membrane ruffles following epidermal growth factor stimulation. J Biol Chem *278*, 11376-11385.
6. Brenner, S. (1974). The genetics of *Caenorhabditis elegans*. Genetics *77*, 71-94.
7. Hodgkin, J. (1983). Male phenotypes and mating efficiency in *Caenorhabditis elegans*. Geneitcs *103*, 43-64.
8. Stinchcomb, D.T., Shaw, J.E., Carr, S.H., and Hirsh, D. (1985). Extrachromosomal DNA transformation of *Caenorhabditis elegans*. Mol Cell Biol *5*, 3484-3496.
9. Bae, Y.K., Lyman-Gingerich, J., Barr, M.M., and Knobel, K.M. (2008). Identification of genes involved in the ciliary trafficking of *C. elegans* PKD-2. Dev Dyn *237*, 2021-2029.
10. Bae, Y.K., Qin, H., Knobel, K.M., Hu, J., Rosenbaum, J.L., and Barr, M.M. (2006). General and cell-type specific mechanisms target TRPP2/PKD-2 to cilia. Development *133*, 3859-3870.
11. Shaner, N.C., Campbell, R.E., Steinbach, P.A., Giepmans, B.N., Palmer, A.E., and Tsien, R.Y. (2004). Improved monomeric red, orange and yellow fluorescent proteins derived from Discosoma sp. red fluorescent protein. Nat Biotechnol *22*, 1567-1572.
12. Mello, C.C., Kramer, J.M., Stinchcomb, D., and Ambros, V. (1991). Efficient gene transfer in C.elegans: extrachromosomal maintenance and integration of transforming sequences. Embo J *10*, 3959-3970.
13. Shakes, D.C., and Ward, S. (1989). Initiation of spermiogenesis in *C. elegans*: a pharmacological and genetic analysis. Dev Biol *134*, 189-200.
14. Barr, M.M., and Sternberg, P.W. (1999). A polycystic kidney-disease gene homologue required for male mating behaviour in *C. elegans*. Nature *401*, 386-389.
15. Peden, E.M., and Barr, M.M. (2005). The KLP-6 Kinesin Is Required for Male Mating Behaviors and Polycystin Localization in *Caenorhabditis elegans*. Current Biology *15*, 394-404.
16. Hart, A. (2005). Behavior. In WormBook, doi/10.1895/wormbook.1.7.1, http://www.wormbook.org
17. Stanfield, G.M., and Villeneuve, A.M. (2006). Regulation of Sperm Activation by SWM-1 Is Required for Reproductive Success of *C. elegans* Males. Current Biology *16*, 252-263.

18. Perkins, L.A., Hedgecock, E.M., Thomson, J.N., and Culotti, J.G. (1986). Mutant sensory cilia in the nematode *Caenorhabditis elegans*. Dev Biol *117*, 456-487.
19. Machaca, K., DeFelice, L.J., and L'Hernault, S.W. (1996). A novel chloride channel localizes to *Caenorhabditis elegans* spermatids and chloride channel blockers induce spermatid differentiation. Dev Biol *176*, 1-16.
20. Nelson, G.A., and Ward, S. (1980). Vesicle fusion, pseudopod extension and amoeboid motility are induced in nematode spermatids by the ionophore monensin. Cell *19*, 457-464.
21. Ward, S., Hogan, E., and Nelson, G.A. (1983). The initiation of spermiogenesis in the nematode *Caenorhabditis elegans*. Dev Biol *98*, 70-79.
22. Duerr, J.S. (2006). Immunohistochemistry. In WormBook, doi/10.1895/wormbook.1.7.1, http://www.wormbook.org., 2007/12/01 Edition
23. Lang, B.F., O'Kelly, C., Nerad, T., Gray, M.W., and Burger, G. (2002). The closest unicellular relatives of animals. Curr Biol *12*, 1773-1778.
24. Maddison, D.R.a.M.W.P. (2001). MacClade 4: Analysis of phylogeny and character evolution (Sunderland, MA: Sinauer).
25. Swofford, D.L. (2003). PAUP*. Phylogenetic Analysis Using Parsimony (* and Other Methods) (Sunderland, MA: Sinauer).

SF1

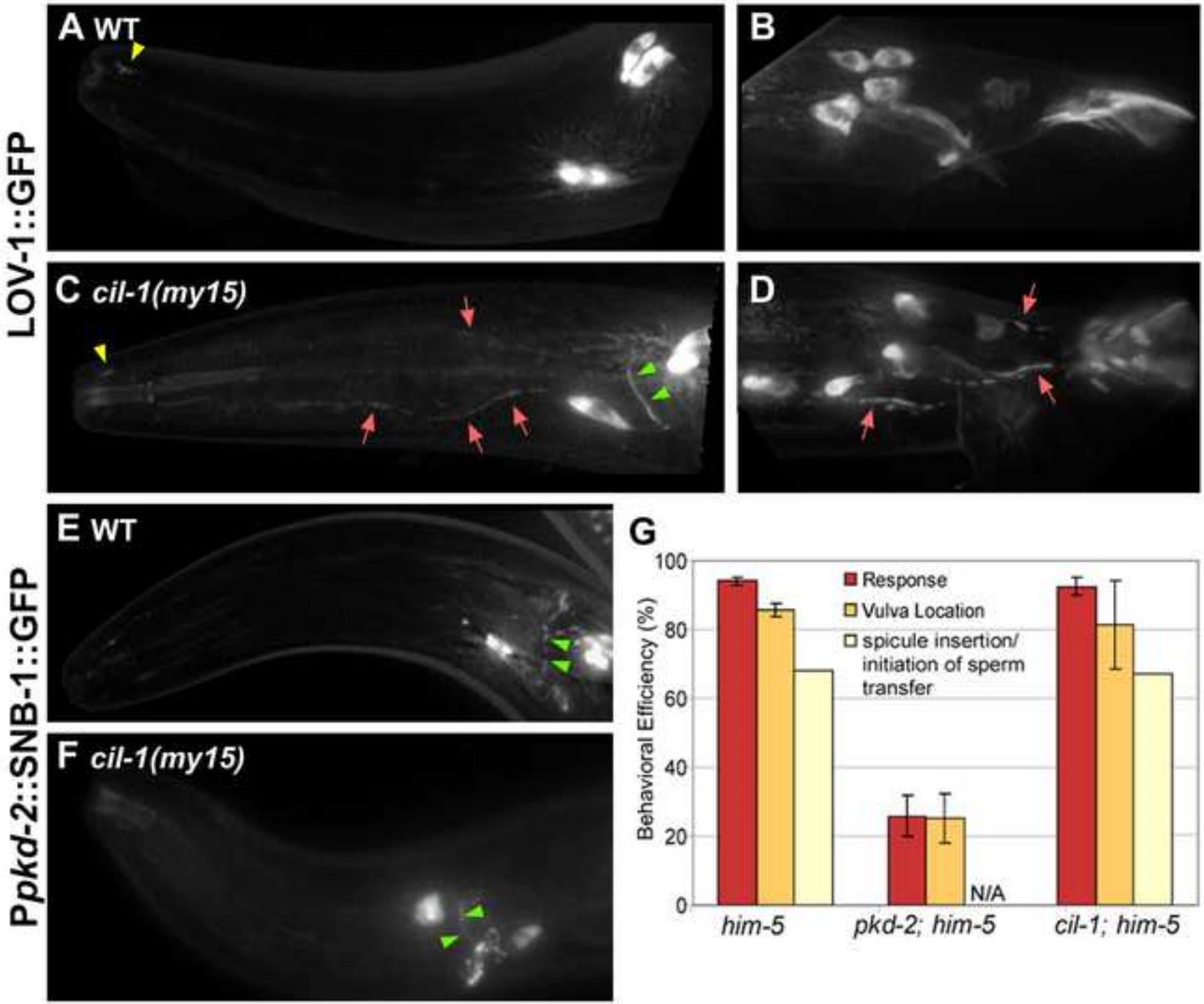
LOV-1::GFP
A WT
B
C cil-1(my15)
D
Ppkd-2::SNB-1::GFP
E WT
F cil-1(my15)
G
Behavioral Efficiency (%)
100
80
60
40
20
0
Response
Vulva Location
spicule insertion/ initiation of sperm transfer
N/A
him-5
pkd-2; him-5
cil-1; him-5

SF2

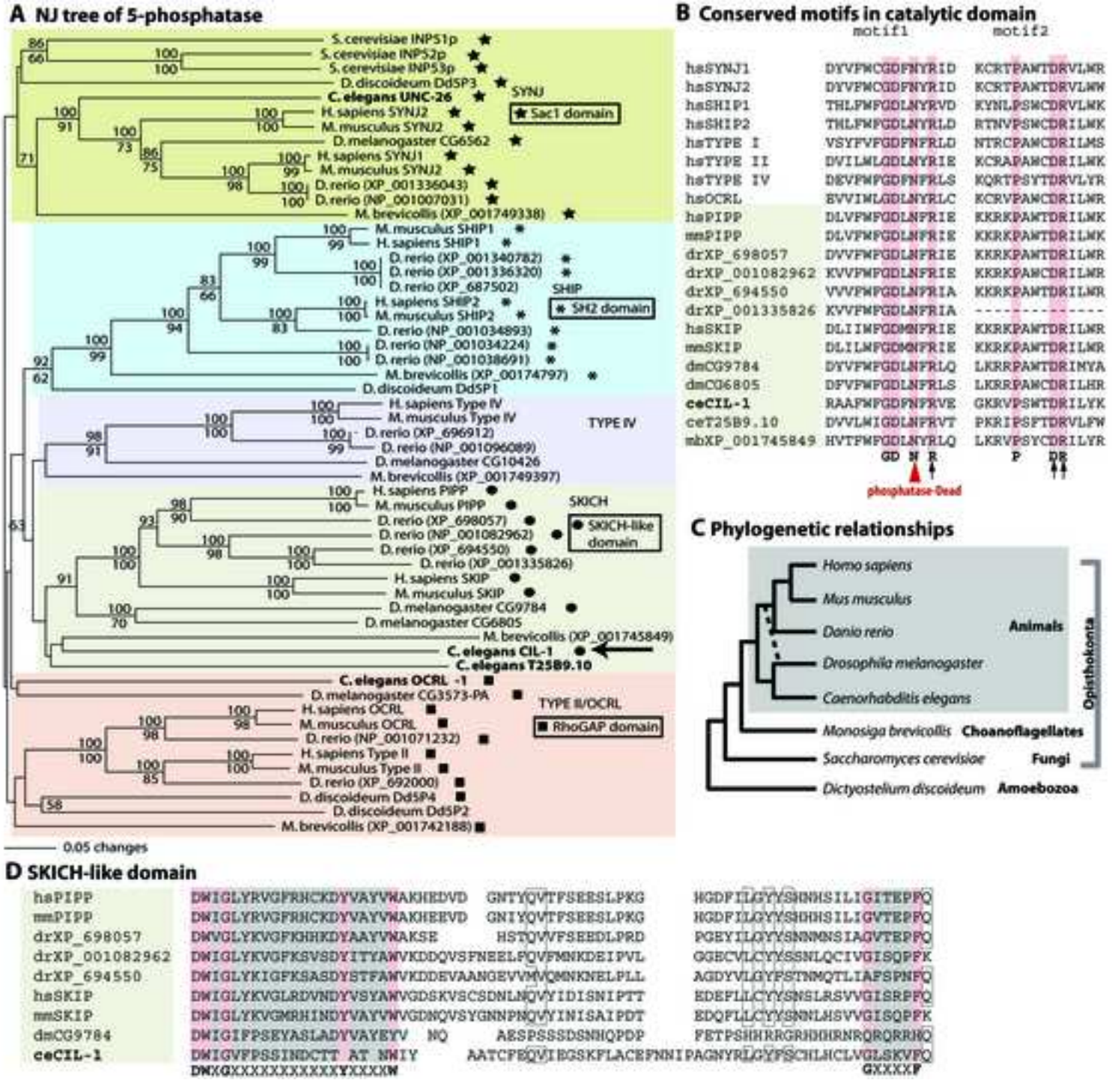
A NJ tree of 5-phosphatase
S. cerevisiae INP51p
S. cerevisiae INP52p
S. cerevisiae INP53p
D. discoideum Dd5P3
C. elegans UNC-26
H. sapiens SYNJ2
M. musculus SYNJ2
D. melanogaster CG6562
H. sapiens SYNJ1
M. musculus SYNJ2
D. rerio (XP_001336043)
D. rerio (NP_001007031)
M. brevicollis (XP_001749338)
SYNJ
Sac1 domain
M. musculus SHIP1
H. sapiens SHIP1
D. rerio (XP_001340782)
D. rerio (XP_001336320)
D. rerio (XP_687502)
H. sapiens SHIP2
M. musculus SHIP2
D. rerio (NP_001034893)
D. rerio (NP_001034224)
D. rerio (NP_001038691)
M. brevicollis (XP_00174797)
D. discoideum Dd5P1
SHIP
SH2 domain
H. sapiens Type IV
M. musculus Type IV
D. rerio (XP_696912)
D. rerio (NP_001096089)
D. melanogaster CG10426
M. brevicollis (XP_001749397)
TYPE IV
H. sapiens PIPP
M. musculus PIPP
D. rerio (XP_698057)
D. rerio (NP_001082962)
D. rerio (XP_694550)
D. rerio (XP_001335826)
H. sapiens SKIP
M. musculus SKIP
D. melanogaster CG9784
D. melanogaster CG6805
M. brevicollis (XP_001745849)
C. elegans CIL-1
C. elegans T25B9.10
SKICH
SKICH-like domain
C. elegans OCRL -1
D. melanogaster CG3573-PA
H. sapiens OCRL
M. musculus OCRL
D. rerio (NP_001071232)
H. sapiens Type II
M. musculus Type II
D. rerio (XP_692000)
D. discoideum Dd5P4
D. discoideum Dd5P2
M. brevicollis (XP_001742188)
TYPE II/OCRL
RhoGAP domain
0.05 changes
B Conserved motifs in catalytic domain
motif1
motif2
hsSYNJ1 DYVFWCGDFNYRID KCRTPAWTDRVLWR
hsSYNJ2 DYVFWCGDFNYRID KCRTPAWTDRVLWW
hsSHIP1 THLFWPGDLNYRVD KYNLPSWCDRVLWK
hsSHIP2 THLFWPGDLNYRLD RTNVPSWCDRILWK
hsTYPE I VSYFVFGDFNFRLD NTRCPAWCDRILMS
hsTYPE II DVILWLGDLNYRIE KCRAPAWCDRILWK
hsTYPE IV DEVPWPGDFNFRLS KQRTPSYTDRVLYR
hsOCRL EVVIWLGDLNYRLC KCRVPAWCDRILWR
hsPIPP DLVFWPGDLNFRIE KKRKPAWTDRILWK
mmPIPP DLVFWPGDLNFRIE KKRKPAWTDRILWK
drXP_698057 DVVFWPGDLNFRIE KKRKPAWTDRILWR
drXP_001082962 KVVFWPGDLNFRIE KKRKPAWCDRILWR
drXP_694550 VVVFWPGDLNFRIA KKRKPAWTDRILWR
drXP_001335826 KVVFWPGDLNFRIA ----------
hsSKIP DLIIWPGDMNFRIE KKRKPAWTDRILWR
mmSKIP DLILWPGDMNFRIE KKRKPAWTDRILWR
dmCG9784 DYVFWPGDLNFRLQ LKRRPAWTDRIMYA
dmCG6805 DFVFWPGDLNFRLS LKRRPAWCDRILHR
ceCIL-1 RAAFWPGDFNFRVE GKRVPSWTDRILYK
ceT25B9.10 DVVLWIGDLNFRVT PKRIPSFTDRVLFW
mbXP_001745849 HVTFWPGDLNYRLQ LKRVPSYCDRILYR
GD N R
P DR
phosphatase-Dead
C Phylogenetic relationships
Homo sapiens
Mus musculus
Danio rerio
Drosophila melanogaster
Caenorhabditis elegans
Animals
Monosiga brevicollis
Choanoflagellates
Saccharomyces cerevisiae
Fungi
Dictyostelium discoideum
Amoebozoa
Opisthokonta
D SKICH-like domain
hsPIPP DWIGLYRVGFRHCKDYVAYVWAKHEDVD GNTYQVTFSEESLPKG HGDFILGYYSHHHSILIGITEPFQ
mmPIPP DWIGLYRVGFRHCKDYVAYVWAKHEEVD GNIYQVTFSEESLPKG HGDFILGYYSHHHSILIGVTEPFQ
drXP_698057 DWVGLYKVGFKHHKDYAAYVWAKSE HSTQVVFSEEDLPRD PGEYILGYYSNNMNSIAGVTEPFQ
drXP_001082962 DWIGLYKVGFKSVSDYITYAWVKDDQVSFNEELFQVFMNKDEIPVL GGECVLCYYSSNLQCIVGISQPFK
drXP_694550 DWIGLYKIGFKSASDYSTFAWVKDDEVAANGEVVWQMNKNELPLL AGDYVLGYFSTNMQTLIAFSPNFQ
hsSKIP DWIGLYKVGLRDVNDYVSYAWVGDSKVSCSDNLNQVYIDISNIPTT EDEFLLCYYSNSLRSVVGISRPFQ
mmSKIP DWIGLYKVGMRHINDYVAYVWVGDNQVSYGNNPNQVYINISAIPDT EDQFLLCYYSNNLHSVVGISQPFK
dmCG9784 DWIGIFPSEYASLADYVAYEYV NQ AESPSSSDSNNQPDP FETPSHHRRGRHGHRNRQRQRRHQ
ceCIL-1 DWIGVFPSSINDCTT AT NWIY AATCFEQVIEGSKFLACEPNNIPAGNYRLGYFSCHLHCLVGLSKVFQ
DWXGXXXXXXXXXXYXXXXW
GXXXXF

SF3

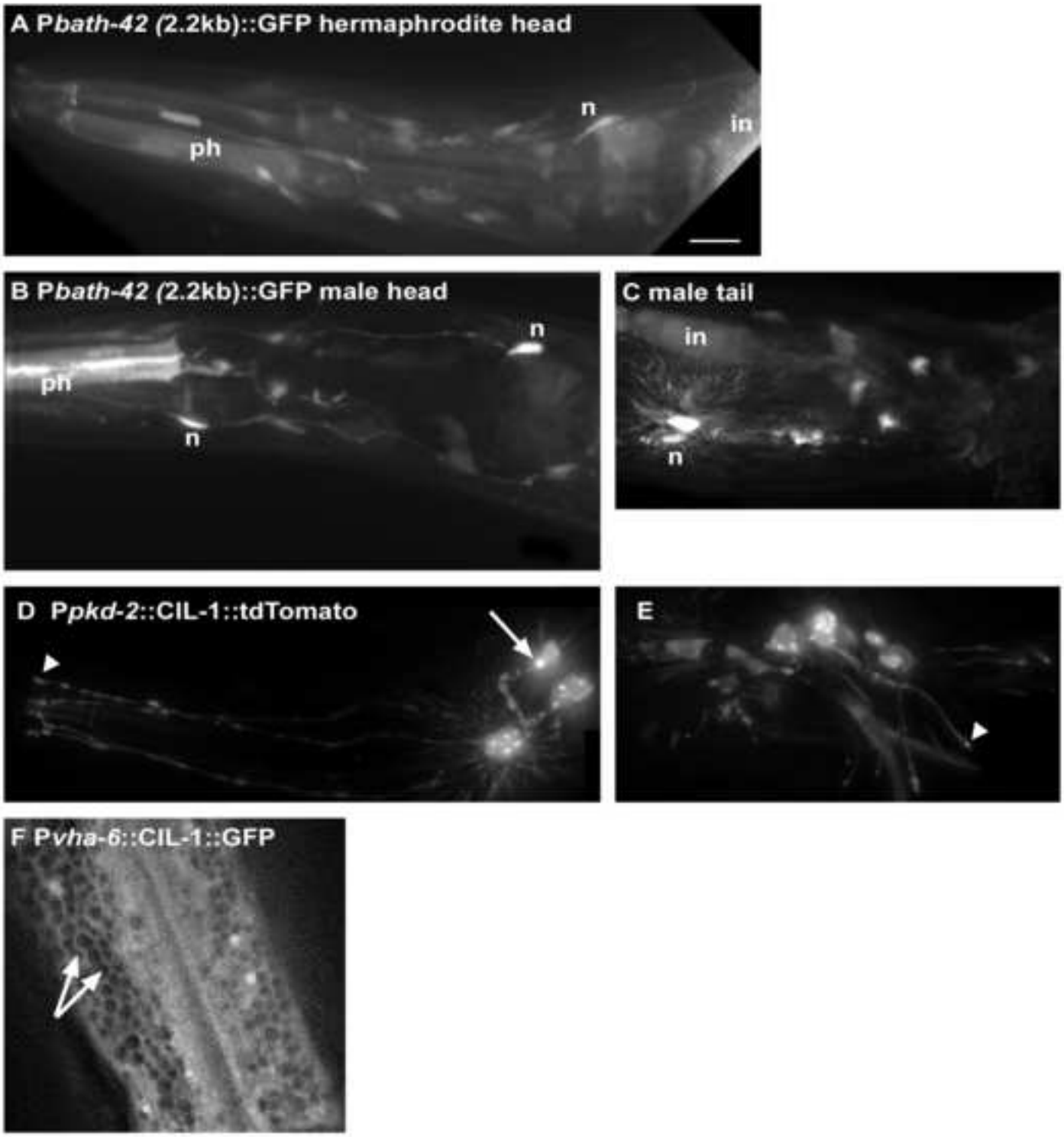
A Pbath-42 (2.2kb)::GFP hermaphrodite head
ph
n
in
B Pbath-42 (2.2kb)::GFP male head
ph
n
n
C male tail
in
n
D Ppkd-2::CIL-1::tdTomato
E
F Pvha-6::CIL-1::GFP

SF4

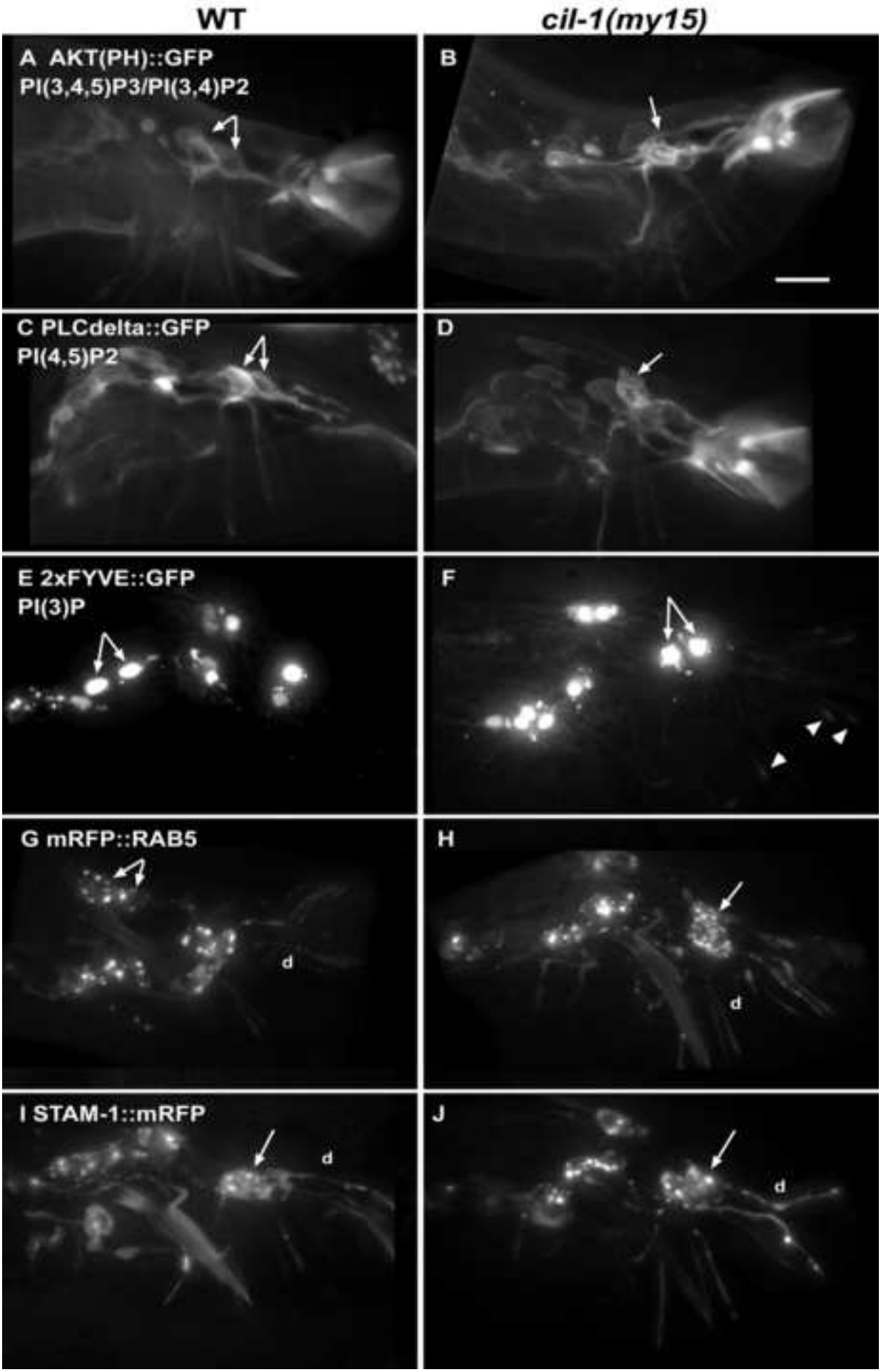
WT
cil-1(my15)
A AKT(PH)::GFP
PI(3,4,5)P3/PI(3,4)P2
B
C PLCdelta::GFP
PI(4,5)P2
D
E 2xFYVE::GFP
PI(3)P
F
G mRFP::RAB5
d
H
d
I STAM-1::mRFP
d
J
d

A brood size

	WT (him-5) ♂ (± sem, n=8)	*cil-1; him-5* ♂ (± sem, n=6)
Average brood size	241.0 ± 9.6	11.7 ± 1.9
Number of unfertilized oocytes	14.4 ± 4.3	216.2 ± 22.6

B hermaphroditic sterility rescue

	dpy-17 cil-1; ♂ *pkd-2 myIs1; him-5* (±sem)		*cil-1; him-5* (±sem) ♂	
	ME (%) (cross/total)	total progeny	ME (%)	total progeny
♂ *WT (him-5)* (n=5)	94.6 ± 1.9	327.4 ± 62.1	NA	NA
♂ *him-5 myIs4* (n=4)	94.1 ± 1. 1	228.8 ± 13.4	91.6 ± 0.5	206.5 ± 48.5

C male infertility

	dpy-17 (± sem) ♂	
	ME (%)	total progeny
♂ *WT (him-5)* (n=5)	58.3 ± 5.9	502.2 ± 97.0
♂ *cil-1; him-5* (n=5)	1.9 ± 0.8	436.8 ± 53.5